S100A6 is a potential diagnostic and prognostic biomarker for human glioma

BO HONG[1], HUI ZHANG[1], YUFEI XIAO[2], LINGWEI SHEN[2] and YUN QIAN[3]

Departments of [1]Pathology and [2]Clinical Laboratory, The Second Affiliated Hospital, Zhejiang University School of Medicine, Hangzhou, Zhejiang 310009; [3]Department of Clinical Laboratory, Stomatology Hospital, School of Stomatology, Zhejiang University School of Medicine, Zhejiang Provincial Clinical Research Center for Oral Diseases, Key Laboratory of Oral Biomedical Research of Zhejiang Province, Cancer Center of Zhejiang University, Hangzhou, Zhejiang 310006, P.R. China

Abstract. S100 calcium-binding protein A6 (S100A6) is a protein that belongs to the S100 family. The present study aimed to investigate the function of S100A6 in the diagnosis and survival prediction of glioma and elucidated the potential processes affecting glioma development. The Cancer Genome Atlas database was searched to identify the relationship among S100A6 expression, immune cell infiltration, clinicopathological parameters and glioma prognosis. Several clinical cases were used to verify these findings. S100A6 gene expression was high in glioma tissues, suggesting its diagnostic significance. In particular, S100A6 upregulation in glioma tissues exhibited a significant and positive correlation with the World Health Organization (WHO) grade, histological type, age, sex, primary treatment outcomes, 1p/19q codeletion, isocitrate dehydrogenase (IDH) status, overall survival (OS), progression-free interval and disease-specific survival. Kaplan-Meier and Cox regression analyses revealed that S100A6 gene expression can independently function as a risk factor affecting the prognosis of patients with glioma. Furthermore, Gene Ontology functional enrichment analysis revealed that S100A6 is implicated in immune responses and that the expression profiles of S100A6 are linked to the immune microenvironment. Furthermore, immunohistochemistry revealed that increased S100A6 protein levels are correlated with age, 1p/19q codeletion, IDH status, WHO grade and OS. The present findings suggest that increased S100A6 expression is an indicator of the dismal prognosis of patients with glioma and that it can be used as a potential diagnostic biomarker for this condition.

Correspondence to: Dr Yun Qian, Department of Clinical Laboratory, Stomatology Hospital, School of Stomatology, Zhejiang University School of Medicine, Zhejiang Provincial Clinical Research Center for Oral Diseases, Key Laboratory of Oral Biomedical Research of Zhejiang Province, Cancer Center of Zhejiang University, 166 North Qiutao Road, Hangzhou, Zhejiang 310006, P.R. China
E-mail: qianyun1985@zju.edu.cn

Introduction

Gliomas are specific tumour types present in either the brain or the spinal cord. Notably, gliomas start in the gluey supportive cells, called glial cells, that surround nerve cells and help in their functioning. Gliomas are one of the most prevalent types of brain tumours and most cancerous tumours found in the brain and central nervous system are gliomas (1). Based on the criteria established by the World Health Organization (WHO), gliomas may have different severity levels, from grade I to IV (2). At present, surgical resection combined with radiotherapy, chemotherapy and targeted therapy are the primary clinical treatment strategies for gliomas (3). However, owing to the high heterogeneity and invasiveness of gliomas, complete surgical resection of the focus is challenging; furthermore, drugs cannot pass through the blood-brain barrier, severely limiting the efficacy of traditional therapeutic drugs, including immunotherapy, targeted therapy and chemotherapy (4). Therefore, the survival time of most patients with gliomas is markedly short and patients with high-grade gliomas have the lowest 5-year survival rate of ~5.4% among all cancer types (3,5).

Recent advances in molecular biology and molecular pathology as well as detailed studies on key molecules and signalling pathways involved in tumorigenesis and development have led to the development of targeted therapies for corresponding molecular targets and signalling pathways, including epidermal growth factor receptor tyrosine kinase inhibitors, anti-vascular endothelial growth factor therapy and mutant isocitrate dehydrogenase (IDH) as molecularly targeted drugs (6-9). Furthermore, molecular pathology, a new concept, has again been elevated to a new level in the 2021 WHO diagnosis and treatment guidelines (10). These new guidelines for glioma diagnosis and treatment are not only related to the classification, diagnosis and prognostic evaluation of gliomas but also to the grading, optimization and updating of the traditional morphological classification methods for gliomas.

This new classification method, involving molecular typing as the core basis for tumour classification, not only increases the accuracy and reliability of diagnosis but also helps accurately judge prognosis and guide treatment, making it a revolutionary approach (10). Therefore, it is vital to explore new and reliable molecular markers for glioma diagnosis and prognosis in the future to clinically manage patients with this condition.

S100 Calcium-binding protein A6 (S100A6) is a protein that belongs to the S100 family; it plays a role in tumour occurrence and progression by promoting the epithelial-mesenchymal transformation, proliferation and migration of several cancer cells (11-14). In addition, S100A6 is associated with the unfavourable prognosis of patients with cancer (15). However, a previous study reported that S100A6 expression is remarkably decreased in non-small cell lung cancer tissues compared with that in normal tissues (16); these findings suggest that S100A6 plays different roles in different tumours. Previous studies reported that the clinical significance of S100A6 in gliomas is controversial. Camby *et al* (17) reported that S100A6 protein levels can help clearly distinguish between low- and high-grade astrocytomas. However, another study reported that S100A6 is highly expressed in human astrocytomas; however, its expression does not exert significant functional changes in the degree of malignancy of the tumour (18). Therefore, S100A6 cannot be used as a specific marker among different grades. Kucharczak *et al* (19) reported that gastrin can mediate the movement of glioblastoma cells by upregulating the promoter of S100A6, which could induce the overexpression of S100A6. To the best of our knowledge, the correlation between S100A6 and glioma is inconclusive, with only the study by Zhang *et al* (20) suggesting that S100A6 upregulation in low-grade glioma is markedly correlated with a dismal prognosis. However, at present, studies on the biological function of S100A6 in gliomas are lacking and the diagnostic and prognostic significance of S100A6 in gliomas should be further validated. Therefore, additional studies are warranted to determine the clinical significance of S100A6 in gliomas.

In the present study, the Genotype-Tissue Expression (GTEx) and The Cancer Genome Atlas (TCGA) databases were used to elucidate the clinical significance of S100A6 in glioblastoma. Moreover, the present study confirmed this significance in a small clinical cohort of glioma. The present findings enhance the understanding of the role of S100A6 in glioblastoma and should help in the detection of this protein, assess its clinical importance and prognostic significance and develop new therapeutic approaches for patients with glioma.

Materials and methods

Data collection and analysis. Information on S100A6 gene expression and the basic clinical characteristics of 33 tumour types were derived from GTEx and TCGA (https://portal.gdc.cancer.gov) (21-23). TCGAbiolinks (R package; https://bioconductor.org/packages/TCGAbiolinks/) was used to download and organise the RNA sequencing (RNA-seq) data and clinical information for each representative tumour type from TCGA and convert them into the TPM format for subsequent analysis. Simultaneously, UCSCXenaTools (R package;, https://ucsc-public.xenahubs.net) was used to download the RNA-seq data and clinical information for normal individuals from the GTEx project database (https://gtexportal.org/home/). RNAseq data through Spliced Transcripts Alignment to a Reference comparison process of 33 tumor projects, TCGA-Glioblastoma Multiforme and TCGA-Low Grade Glioma projects were downloaded and collated from TCGA database (24). After determining the differential expression of the S100A6 gene, the findings were expressed as a box diagram and a paired difference diagram.

Differential gene expression, link and enrichment analyses. DESeq2 (R package; https://bioconductor.org/packages/DESeq2/) was used to compare S100A6 expression data (HTseq count) (critical value=50%) and identify the differentially expressed genes (DEGs) [fold change (FC) >2.0 or <−2.0, P<0.05] (25). Ggplot2 (R package; https://ggplot2.tidyverse.org) was used to plot the heatmaps of the top 10 DEGs. Based on the data from TCGA-Stomach Adenocarcinoma, Pearson's link analysis of S100A6 mRNA and other glioma-related mRNAs was conducted. Furthermore, to determine the function of S100A6, the top 300 genes that had the strongest positive association with S100A6 were subjected to enrichment analysis.

To elucidate the biological role of S100A6 in glioma development, ClusterProfiler (R package; https://bioconductor.org/packages/clusterProfiler/) was used to perform gene set enrichment analysis (GSEA) using the Kyoto Encyclopedia of Genes and Genomes (KEGG), Gene Ontology (GO) and protein-protein interaction (PPI) datasets. Enrichplot (R package; https://bioconductor.org/packages/enrichplot/) was used to illustrate the top five signalling pathways that had the highest significance level of enrichment in the database (26).

Single-sample (ss)GSEA to evaluate immune cell infiltration. The median expression of the S100A6 gene was used to divide TCGA glioma samples into high- and low-expression groups. The infiltrating immune cell levels were compared between the two groups. The immune infiltration landscape was investigated using the ssGSEA algorithm. Furthermore, Spearman's link analysis was performed to elucidate the relationship between S100A6 expression profiles and infiltrating immune cell subpopulations. Immune cells with an R-value >0.4 or <−0.4 were selected for the scatter plots and chord plots were generated.

Patients and tissue samples. In total, 43 patients with glioma who had undergone surgical resection between January 2016 and October 2017 at the Second Affiliated Hospital of Zhejiang University School of Medicine were included in the present study. Glioma samples and their associated medical information were obtained from all patients. The inclusion criteria were as follows: i) glioma primary tumour; ii) histopathological confirmation of glioma diagnosis; iii) received preoperative chemo-radiotherapy; and iv) complete clinical records. The exclusion criteria were as follows: i) autoimmune disorders or other diseases; ii) other severe diseases; and iii) previous immunosuppressive schemes. The present study adhered to the ethical principles outlined in The Declaration of Helsinki. Study procedures were approved by the Ethics Committee of the Second Affiliated Hospital of Zhejiang University School of Medicine, Hangzhou, China (approval no: 2021-0641).

Immunohistochemical (IHC) staining. Glioma tissue blocks were fixed in 10% formalin at room temperature and embedded in paraffin before they were sliced into 5-mm thick sections for IHC staining. The slides were deparaffinized with xylene and rehydrated using a series of successively increasing alcohol dilutions (absolute ethanol, 95% ethanol, 80% ethanol, 70% ethanol and 50% ethanol) at room temperature. Subsequently, the slices were treated with 0.3% hydrogen peroxide at 25°C for 30 min to inhibit endogenous peroxidase activity. Thereafter, to retrieve the antigens, the sections were boiled for 30 min in citrate buffer (10 mmol/l; Ph 6.0) at 100°C. Non-specific binding was prevented by incubating the slides with 10% normal goat serum (cat. no. ZLI-9022; OriGene Technologies, Inc.) for 10 min after washing the slides three times with phosphate-buffered saline, 5 min each time. Thereafter, the slides were incubated with rabbit anti-human S100A6 monoclonal antibody (1:200; cat. no. ab250543; Abcam) at 4°C overnight. Immunoassay was conducted as previously described using the Dako EnVision detection system (K5007, Dako; Agilent Technologies, Inc.) (27). Mayer's haematoxylin was used as the counterstaining agent for 8 min at room temperature. Slides were dehydrated using serial dilutions of alcohol (50% ethanol, 70% ethanol, 80% ethanol, 95% ethanol and absolute ethanol). Finally, the slides were mounted in neutral resin.

Manual IHC staining quantitation. Two different pathologists who were blinded to the clinical features quantitatively analysed IHC staining results. Based on the number of S100A6-positive cells, the positive cell rate was categorized into five levels: 0 (0%); 1 (1-10%); 2 (10-50%); 3 (50-70%); and 4 (70-100%). Furthermore, based on staining intensity, positive S100A6 expression was categorized into four classes: 0 (no staining); 1 (weak staining in light yellow); 2 (mild staining in yellow brown); and 3 (strong staining in dark brown). A semi-quantitative score was generated by combining the results of the two indicators, i.e. the number of positive cells and staining intensity. The product of these two indicators was used to provide the final IHC score (0-12). IHC staining was performed to categorize the tissue staining pattern as either high (IHC score=4-12) or low (IHC score=0-3) expression (26).

Prognostic analyses. Kaplan-Meier (K-M) analysis was the foundation for plotting the overall survival (OS) curve. Patients were grouped based on the expression of S100A6 and labeled with their survival status and OS time. The K-M analysis was conducted using R software (R package; https://CRAN.R-project.org/package=survival), with the logrank test for comparison. The K-M survival curve was plotted using Graphpad Prism 10 software (https://www.graphpad-prism.cn/). Furthermore, OS was determined using univariate and multivariate Cox regression models by focusing on the effects of the S100A6 gene and clinical factors on patient outcomes. WHO grade, IDH status and 1p/19q codeletion information provided by Ceccarelli *et al* (24) were downloaded; furthermore, the prognostic data provided by Liu *et al* (28) were downloaded. After removing the samples with missing clinical information, the survival function (R package; https://CRAN.R-project.org/package=survival) was used for proportional risk hypothesis testing, followed by Cox

regression analysis. Lastly, rms (R package; https://hbiostat.org/R/rms/) was used to construct a nomogram for regression analysis.

Statistical analyses. Statical and bioinformatics analyses were conducted using R software (version Rx64 V3.6.3; https://cran.r-project.org).The pROC (R package; https://bioconductor.org/packages/ROC/) was used to construct the receiver operating characteristic (ROC) curves and visualize them. The area under the ROC (AUC) was determined and the AUC value was calculated. It is generally believed that AUC values between 0.5 and 0.7 indicate low diagnostic accuracy, between 0.7 and 0.9 indicate medium diagnostic accuracy, and above 0.9 indicate high diagnostic accuracy (29). The Wilcoxon rank-sum test was performed to investigate the differential gene expression of S100A6 in glioma tissues and normal brain tissues. Furthermore, the Kruskal-Wallis test, logistic regression analysis and Wilcoxon rank sum test were conducted to verify the relationship between S100A6 gene expression and clinicopathological characteristics. Patients without sufficient clinical information were excluded. The statistical significance of the variations was evaluated using the unpaired Student's t-test, Spearman's link analysis, χ^2 test and Fisher's exact test, as appropriate, for comparing the various groups. P<0.05 was considered to indicate a statistically significant difference.

Results

S100A6 expression is high in glioma tissues. The Wilcoxon rank sum test was performed to determine the differences in the mRNA expression of S100A6 in various cancerous and normal tissues; the findings were based on the data from both GTEx and TCGA (Fig. 1A and B). The S100A6 gene was expressed in various cancers, such as bladder urothelial carcinoma, breast invasive carcinoma, cholangiocarcinoma, colon adenocarcinoma, esophageal carcinoma, head and neck squamous cell carcinoma, kidney chromophobe, kidney renal clear cell carcinoma, kidney renal papillary cell carcinoma, liver hepatocellular carcinoma, lung squamous cell carcinoma, prostate adenocarcinoma, stomach adenocarcinoma and thyroid carcinoma. Furthermore, S100A6 gene expression was increased in glioma tumour tissues compared with that in normal tissue samples (P<0.001; Fig. 1C).

ROC curves are used to determine whether a certain factor has a diagnostic value for a certain disease. Furthermore, AUC reflects the value of the diagnostic tests. The larger the AUC, the higher the diagnostic value. Based on the data from GTEx and TCGA, the ROC curves revealed that the mRNA of S100A6 had an improved diagnostic value in differentiating between normal brain and glioma tissues (AUC=0.830; Fig. 1D).

Association between S100A6 gene expression and the clinicopathological characteristics of patients with glioma. The clinical data that were used to define 696 individuals diagnosed with glioma were retrieved from TCGA and then classified into the low and high groups based on median S100A6 gene expression. To determine the relationship between S100A6 gene expression and the clinicopathological characteristics of patients with glioma, the Wilcoxon rank sum test and logistic regression analysis were performed. Table SI comprehensively
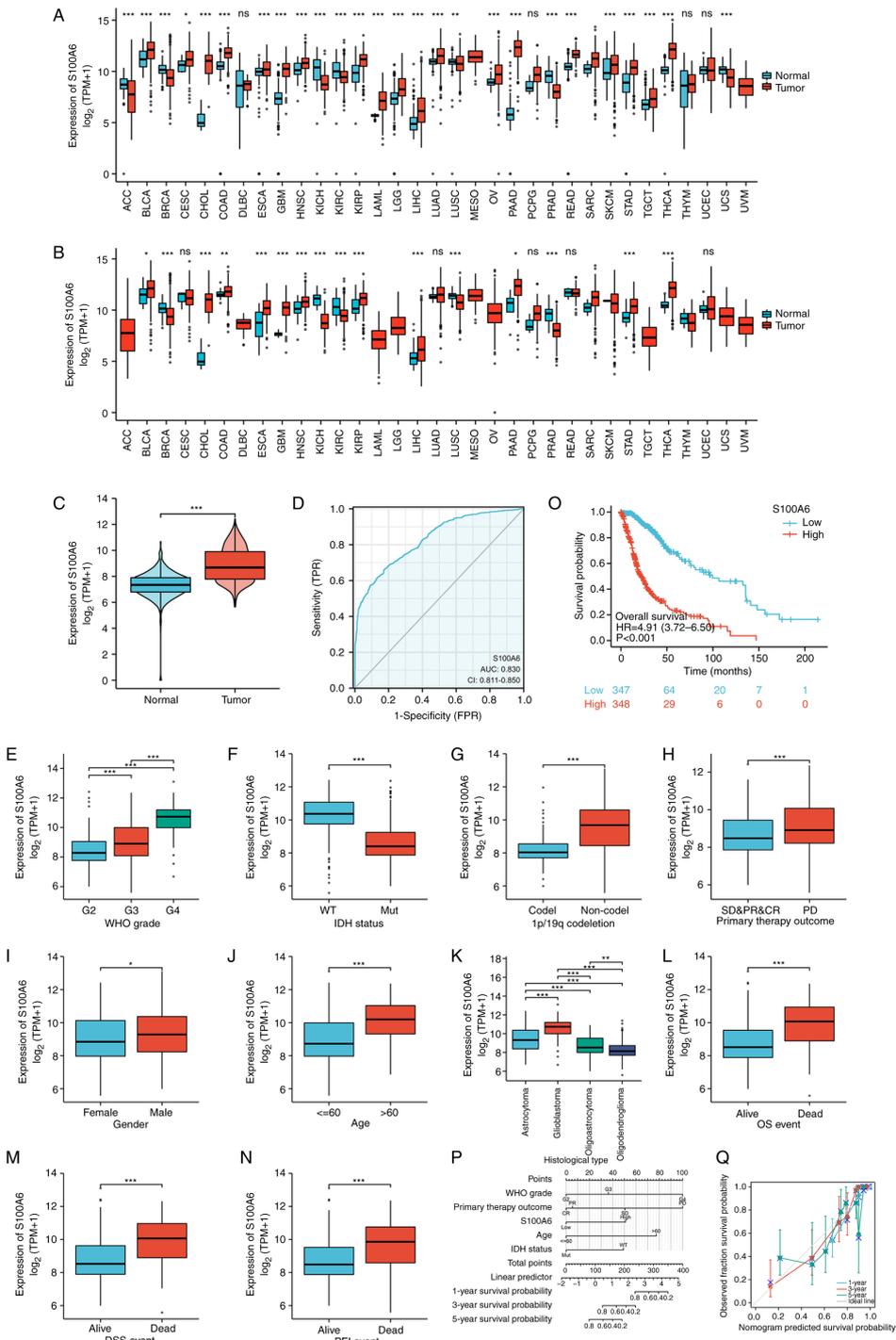
Figure 1. S100A6 levels were increased in glioma tissues compared with those in the adjacent normal tissues and were associated with clinicopathological characteristics. (A) S100A6 expression was shown to be higher or lower in several malignancies compared with that in normal tissues using the GTEx-derived data. (B) Various malignancies in the TCGA database showed either increased or reduced S100A6 expression levels relative to normal tissues. (C) When comparing cancer tissues with normal tissues, the former showed increased S100A6 expression levels. (D) The value of S100A6 gene expression for glioma diagnosis was analyzed using receiver operating characteristic curve plots based on GTEx and TCGA data. S100A6 gene expression in relation with (E) WHO grade, (F) IDH status, (G) 1p/19q codeletion, (H) Primary therapy outcome, (I) Sex, (J) Sge, (K) Histological type and (L) OS, (M) DSS event and (N) PFI events. (O) Survival analysis of S100A6 gene expression in patients with glioma. S100A6 high- and low-expression patient groups were separated using the median score. (P and Q) A prognostic model of S100A6 gene expression in glioma. (P) Prediction of 1-, 3-, and 5-year OS in patients with glioma using a nomogram; (Q) Nomogram calibration plot for predicting 1-, 3-, and 5-year OS rates. ACC, adrenocortical carcinoma; BLCA, bladder urothelial carcinoma; BRCA, breast invasive carcinoma; CESC, cervical squamous cell carcinoma and endocervical adenocarcinoma; CHOL, cholangiocarcinoma; COAD, colon adenocarcinoma; DLBC, lymphoid neoplasm diffuse large B-cell lymphoma; ESCA, esophageal carcinoma; GBM, glioblastoma multiforme; HNSC, head and neck squamous cell carcinoma; KICH, kidney chromophobe; KIRC, kidney renal clear cell carcinoma; KIRP, kidney renal papillary cell carcinoma; LAML, acute myeloid leukemia; LGG, brain lower grade glioma; LIHC, liver hepatocellular carcinoma; LUAD, lung adenocarcinoma; LUSC, lung squamous cell carcinoma; MESO, mesothelioma; OV, ovarian serous cystadenocarcinoma; PAAD, pancreatic adenocarcinoma; PCPG, pheochromocytoma and paraganglioma; PRAD, prostate adenocarcinoma; READ, rectum adenocarcinoma; SARC, sarcoma; SCKM, skin cutaneous melanoma; STAD, stomach adenocarcinoma; TGCT, testicular germ cell tumor; THCA, thyroid carcinoma; THYM, thymoma; UCEC, uterine corpus endometrial carcinoma; USC, uterine carcinosarcoma (UCS); UVM, uveal Melanoma; IDH, isocitrate dehydrogenase; OS, overall survival; DSS, disease-specific survival; PFI, progression-free interval. *P<0.05, **P<0.01, and ***P<0.001.
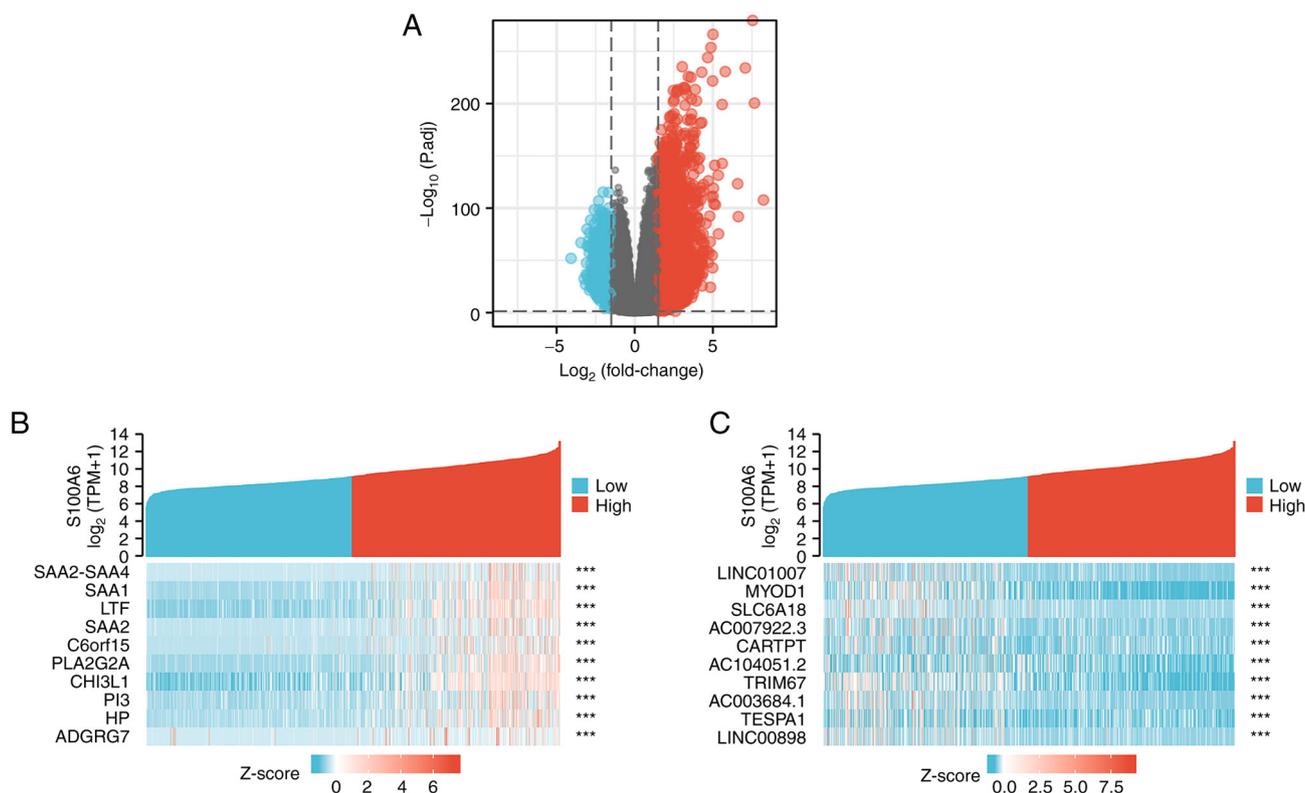
Figure 2. Differential expression genetic map and gene set enrichment analysis in glioma samples with low/high S100A6 expression. (A) Volcano plot showing 1725 upregulated (logFC>2.0, P<0.05) and 273 downregulated (logFC<-2.0; P<0.05) genes. Heatmap of the top 10 most (B) Upregulated and (C) Downregulated genes in the low and high expression groups. Data were normalized by z-score, with the X-axis representing samples and the Y-axis representing differentially expressed genes. Blue and red shades signify down- and upregulated genes, respectively. ***P<0.001.

presents these clinical findings. S100A6 gene expression in glioma was substantially associated with WHO grade, histological type, sex, age, primary treatment outcomes, 1p/19q codeletion, IDH status, OS, disease-specific survival and progression-free interval (P<0.05, Fig. 1E-N). Subsequently, univariate logistic regression analysis was performed to determine the relationship between S100A6 gene expression and the clinicopathological characteristics of patients with glioma. A significant correlation was observed between the S100A6 gene and histological type, age, IDH status, 1p/19q codeletion and WHO grade. However, no association was observed between S100A6 gene expression and primary treatment outcomes, sex and race (Table SII).

Clinical significance of S100A6 gene expression in glioma prognosis. The clinical significance of S100A6 gene expression in terms of glioma prognosis was assessed using the KM plotter database. The high S100A6 gene expression group exhibited a shorter OS than the low-expression group (P<0.001; Fig. 1O). Univariate analysis revealed that S100A6 upregulation was associated with a higher risk of developing glioma [hazards ratio (HR), 4.914; CI, 3.716-6.496; P<0.001; Table SIII). Furthermore, multivariate analysis revealed that increased S100A6 expression was an independent prognostic marker for predicting OS (HR, 2.155; CI, 1.358-3.419; P=0.001; Table SIII).

A nomogram model based on Cox regression analysis results was developed to improve the prognosis of patients diagnosed with glioma (Fig. 1P). The model included four independent prognostic factors: S100A6 expression; primary

treatment outcomes; IDH status; and WHO grade. A point system was used to assign scores to these variables depending on the outcomes of multivariate analysis. A straight line was used to identify the points corresponding to the variables. Then, the total number of points that were allotted to each variable was rescaled such that they were between 0 and 100. The total score was determined by summing all the points assigned to each variable in the analysis. The 1-, 3- and 5-year survival rates of patients diagnosed with glioma were determined by drawing a line directly extending from the axis denoting total score to the axis denoting outcome. All observations of patients were consistent with the calibration curve findings of the OS nomogram (Fig. 1Q).

Identification and enrichment analysis of the DEGs in high/low S100A6 expression glioma samples. The median mRNA expression of the genes in the expression profiles of low and high S100A6 expression samples were compared. In total, 1998 DEGs, with 1,725 upregulated and 273 downregulated genes, were identified that were associated with S100A6 expression. S100A6 gene expression was statistically significant between low and high S100A6 expression groups (|logFC|>2.0, P<0.05, Fig. 2A). Fig. 2B and C display the heatmaps presenting the top 10 downregulated and upregulated DEGs between the high and low S100A6 expression groups.

Functional enrichment analysis was performed using the upregulated and downregulated genes to determine the biological classification of the DEGs. GO analysis revealed the substantial enrichment of the upregulated genes in the immune
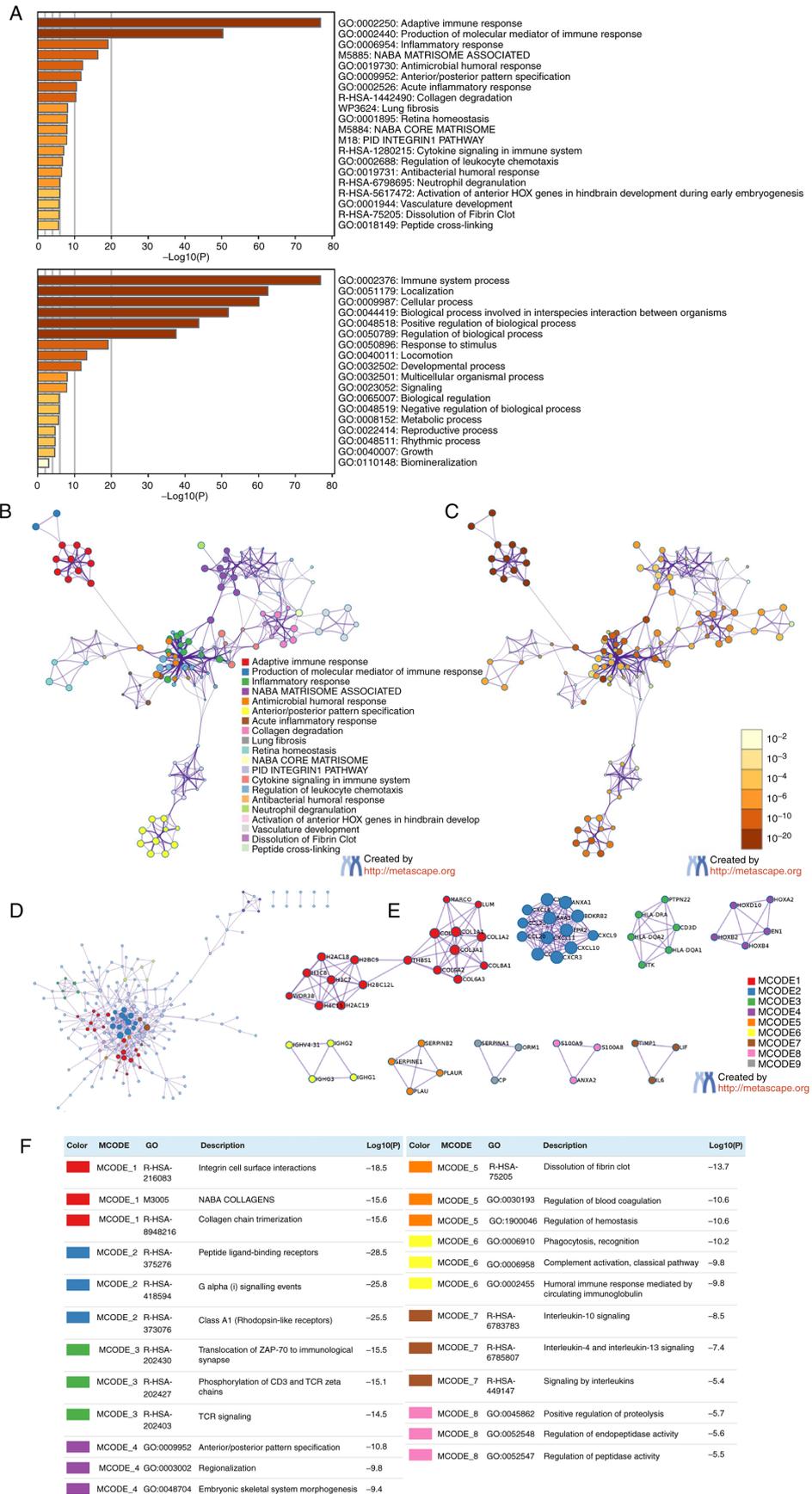
Figure 3. Kyoto Encyclopedia of Genes and Genomes and Gene Ontology enrichment analysis of S100A6-associated upregulated differentially expressed genes in glioma. (A) Bar graph showing enriched terms across upregulated genes, colored by P-values. (B) Colored nodes in the network denote upregulated genes, with nodes sharing the same cluster ID generally located close to one another. (C) A network of enriched terms across upregulated genes, with each term's p-value shown as a different color; terms that include more genes have a more significant p-value. (D) Protein-protein interaction network across upregulated genes. (E) Identification of MCODE components in upregulated gene lists. (F) Description of MCODE components across upregulated genes. GO, Gene Ontology; MCODE, molecular complex detection.
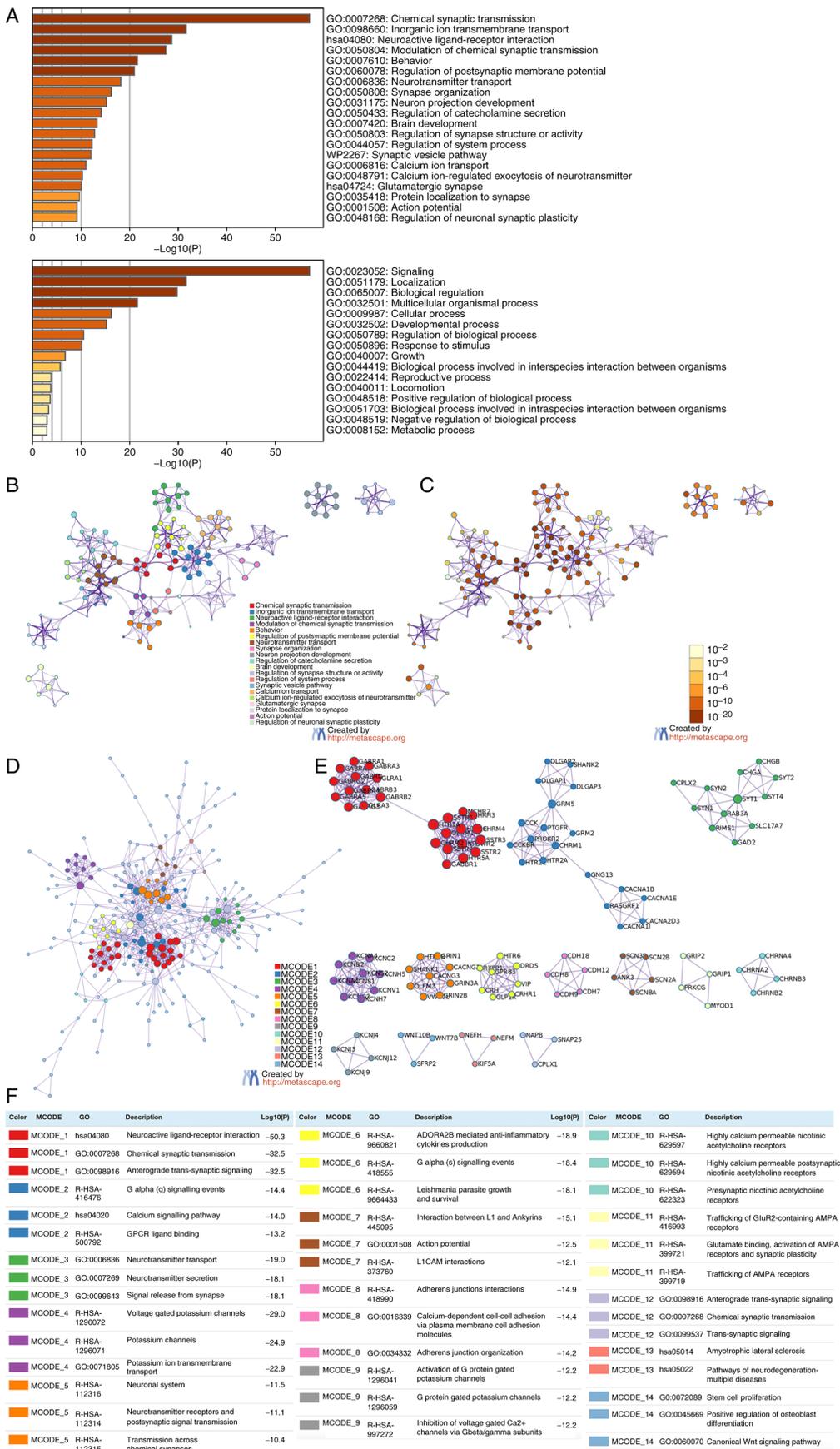
Figure 4. Kyoto Encyclopedia of Genes and Genomes and Gene Ontology analysis of S100A6-associated downregulated differentially expressed genes in glioma. (A) Bar graph showing enriched terms across downregulated genes, colored by P-values. (B) Network of enriched terms across downregulated genes colored by cluster ID, with nodes that belong to the same cluster ID generally located close to one another. (C) A network of enriched terms across downregulated genes, with each term's p-value shown as a different color; terms that include more genes have a more significant p-value. (D) Protein-protein interaction network across downregulated genes. (E) Identification of MCODE components in downregulated gene lists. (F) Description of MCODE components across downregulated genes. GO, Gene Ontology; MCODE, molecular complex detection.
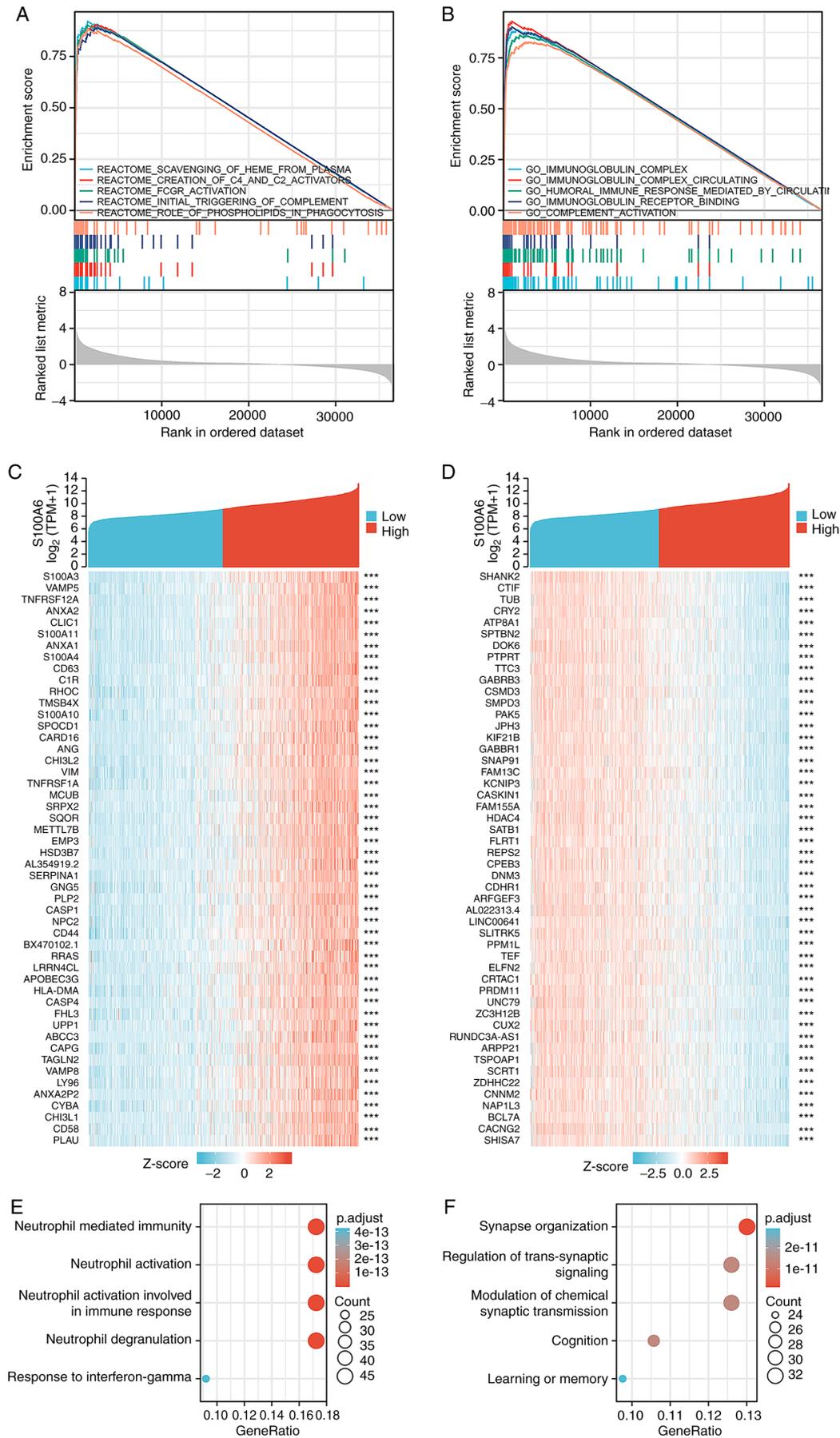
Figure 5. Single gene link enrichment analysis of S100A6. (A and B) Gene set enrichment analysis of S100A6-associated DEGs in glioma. Enrichment analysis of DEGs with S100A6 differentially expressed in (D) C2., cp., v7.2, GMT and (E) C5., all., v7.2, GMT symbols database. Heatmap showing the 50 genes with the highest (C) Positive and (D) Negative correlations. Top 300 genes (E) Positively and (F) Negatively linked to S100A6 according to the list of Gene Ontology terms encompassing biological processes. GMT, Gene Matrix Transposed; DEG, differentially expressed gene.
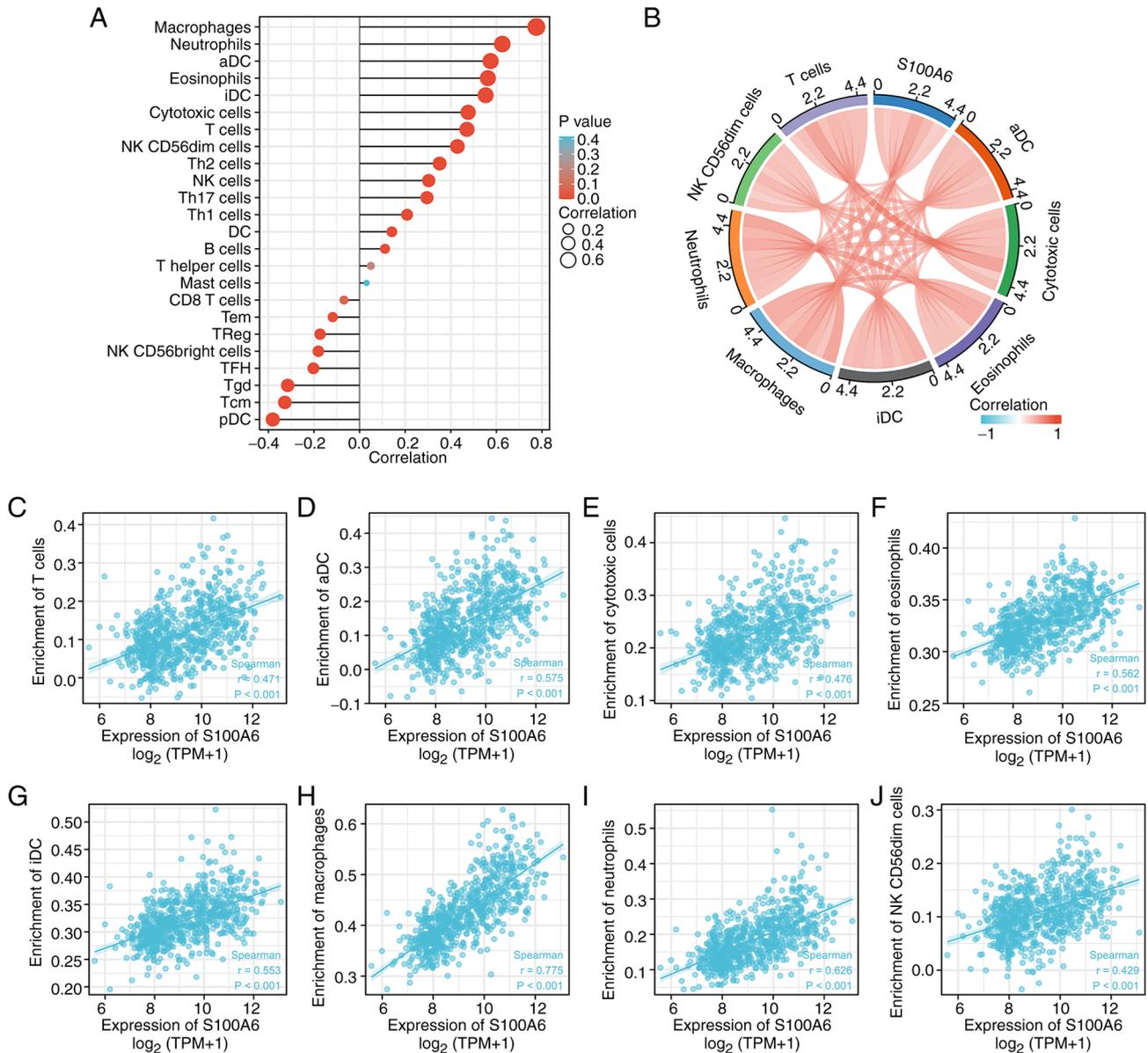
Figure 6. The gene expression of S100A6 was associated with tumor-infiltrating immune cells. (A) S100A6 is correlated with the level of infiltration of immune cells. The absolute value of Spearman's link coefficient is depicted by the size of the dots and the deeper the color, the stronger the link. (B) Chord diagram of the levels of S100A6 gene expression and immune cell infiltration; the red and blue colors correspondingly denote the positive and negative links. A stronger link is indicated by a darker color. (C-J) Association of the S100A6 expression level with the relative abundances of 7 types of immune cells.

system process and synthesis of immune response molecules that act as mediators and adaptive immune response; on the other hand, the downregulated genes were enriched in chemical synaptic transmission, inorganic ion transmembrane transport, chemical synaptic transmission regulation, behaviour and modulation of postsynaptic membrane potential. In addition, KEGG pathway enrichment analysis revealed that the upregulated genes primarily participated in the NABA matrisome-associated pathway (Fig. 3A-C); by contrast, most downregulated genes were implicated in neuroactive ligand-receptor interactions (Fig. 4A-C).

Subsequently, PPI enrichment analysis revealed that the upregulated genes were primarily enriched in integrin cell surface interactions, NABA collagens, collagen chain trimerization, peptide ligand-binding receptors, G alpha signalling events and class A/1 (rhodopsin-like receptors) (Fig. 3D and E).

By contrast, the downregulated genes were primarily enriched in neuroactive ligand-receptor interaction, anterograde trans-synaptic signalling, G alpha signalling events, calcium signalling pathway, chemical synaptic transmission and GPCR ligand binding (Fig. 4D and E). Figs. 3E and F, and 4E and F demonstrate that the MCODE components were identified in the gene lists.

Using TCGA-derived data, GSEA was conducted to investigate the mechanisms underlying the role of the S100A6 gene in glioma. Enrichment data from the Molecular Signatures Database was used to conduct Reactome enrichment analysis and GO enrichment analysis of S100A6 gene expression samples. Reactome enrichment analysis of S100A6 gene expression revealed the top five enriched pathways based on their false discovery rate, normalized enrichment score and P-values: Scavenging

of plasma heme; creation of C2 and C4 activators; Fc gamma receptor activation; initial triggering of complement; and role of phospholipids in phagocytosis (Fig. 5A; Table SIV). Furthermore, the five most enriched GO terms associated with S100A6 gene expression were as follows: Immunoglobulin complex; circulating immunoglobulin complex; humoral immune response mediated by circulating immunoglobulin; immunoglobulin receptor binding; and complement activation (Fig. 5B; Table SIV).

KEGG and GO enrichment analyses of S100A6 expression-associated genes in glioma. Link analysis of S100A with all other mRNAs in glioblastoma was performed using TCGA-derived data to elucidate the activities and pathways affected by S100A in glioma. The top 300 genes that exhibited the strongest positive and negative links with S100A6 were enriched. Fig. 5C and D demonstrates the outcomes of these analyses for the top-ranked genes.

Using the clusterProfiler R tool, the potential functional pathways of S100A6 based on the top 300 genes were elucidated. GO functional enrichment analysis revealed that S100A6 was primarily and positively associated with neutrophil-mediated immunity, neutrophil activation, neutrophil activation involved in immune response, neutrophil degranulation and response to interferon-γ (Fig. 5E). On the other hand, S100A6 was primarily and negatively associated with synapse organisation, regulation of trans-synaptic signalling, modulation of chemical synaptic transmission, cognition and learning or memory (Fig. 5F).

S100A6 gene expression and immune cell infiltration. The immune infiltration algorithm (ssGSEA) and Spearman's correlation were used to determine the relationship between S100A6 expression patterns and invading immune cell subsets using TCGA-derived data of patients with glioma (Fig. 6A). S100A6 expression was positively associated with eosinophils (P<0.001), macrophages (P<0.01), neutrophils (P<0.001), activated dendritic cell (P<0.001), interstitial dendritic cells (P<0.001), cytotoxic cells (P<0.001), T cells (P<0.001) and natural killer CD56^{dim} cells (P<0.001) (immune cells with r>0.4 and P<0.003 selected for description) (Fig. 6B-J). Therefore, elevated S100A6 expression is associated with the intertumoral accumulation of macrophages and neutrophils. These findings suggest an association between the immune state of gliomas and increased S100A6 expression.

Statistical association between S100A6 and the clinicopathological characteristics of patients with glioma in a clinical cohort. In most glioma cases, the S100A6 protein was diffusely expressed in the tumour cell membrane and/or cytoplasm (Fig. 7A). Table I presents the association between the clinicopathological characteristics of 43 patients with glioma and their S100A6 protein levels. Patients with high S100A6 expression had fewer IDH mutations, fewer 1p/19q chromosomal deletions and worse survival (P<0.05). To some extent, these data suggest that enhanced S100A6 expression is associated with tumour progression and that S100A6 performs a critical function in glioma prognosis.

S100A6 protein level and its prognostic significance. The resection date was the starting point for patient follow-up,
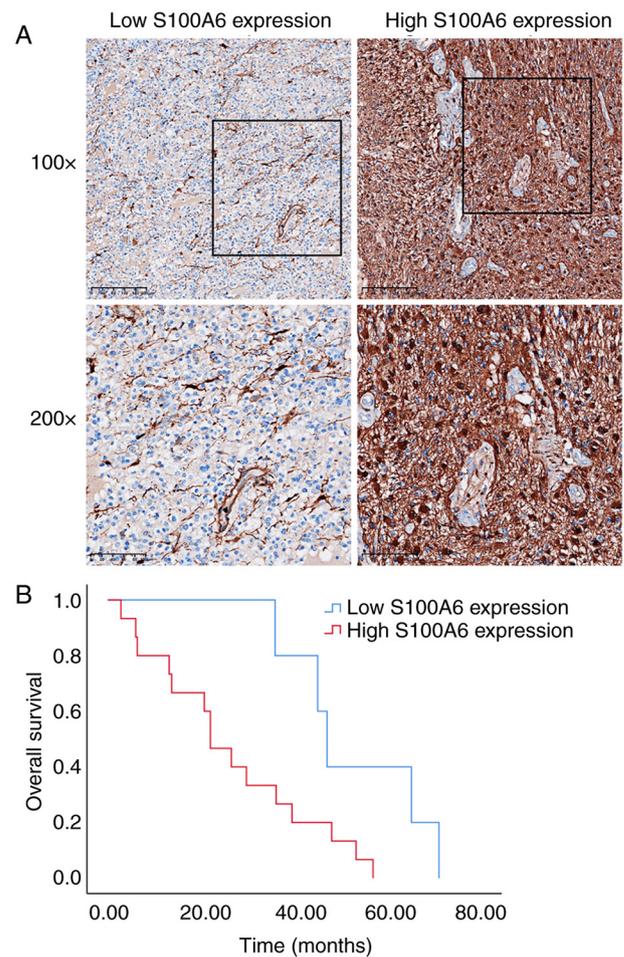

Figure 7. S100A6 expression in a clinical cohort of glioma patients and an analysis of survival. (A) Representative images of S100A6 staining in glioma tumor cells. Original magnification, x100 and x200. (B) K-M plot for glioma patients whose S100A6 expression is high (red line) or low (blue line) (P<0.05).

which continued till October 2022. The date at which survival or death was definitively established was considered the end of OS. The predictive value of S100A6 was determined via KM survival analysis. Fig. 7B demonstrates that the expression profile of the S100A6 protein was correlated with the prognosis of patients with glioma. Furthermore, increased S100A6 levels were associated with decreased OS compared with that in patients with decreased S100A6 levels (P<0.05). The Cox proportional hazard ratio model was used to investigate the potential predictors of OS in patients with glioma. The univariate analysis confirmed that age, WHO stage, IDH mutation, 1p/19q deletion and S100A6 expression were prognostic factors for glioma (Table II). These data suggest that the dismal prognosis of patients with glioma can be predicted by increased S100A6 expression in glioma tissue. This finding may motivate the development of novel therapeutic approaches.

Discussion

Glioma is an extremely aggressive type of brain tumour with poor responses to standard cancer treatment regimens owing to its diffuse infiltration (27). Although there have been advances in the last two decades in understanding glioma pathophysiology

Table I. Association between clinicopathological features and S100A6 expression in glioma patients.

Characteristic	Low expression of S100A6	High expression of S100A6	P-value	S100A6 expression scores, mean ± standard deviation	t	P-value
Number of patients	13	30	-			
World Health Organization grade, n (%)						
G1 + G2	4 (9.30)	5 (11.63)	0.417[b]	6.89±3.95	0.584	0.336
G3 + G4	9 (20.93)	25 (58.14)		6.26±3.48		
Isocitrate dehydrogenase status, n (%)						
Wild type	1 (2.33)	16 (37.21)	0.006[a]	7.82±3.47	2.484	0.017
Mutant	12 (27.91)	14 (32.56)		5.27±3.18		
1p/19q codeletion, n (%)						
Codel	10 (23.26)	9 (20.93)	0.007[a]	5.00±3.45	2.235	0.031
Non-codel	3 (6.98)	21 (48.84)		7.29±3.25		
Years of age, n (%)						
≤60	13 (30.23)	20 (46.51)	0.020[b]	5.88±3.48	1.379	0.175
>60	0	10 (23.26)		7.60±3.37		
Sex, n (%)						
Female	6 (13.95)	14 (32.56)	1.000[a]	6.70±3.73	0.733	0.468
Male	7 (16.28)	16 (37.21)		5.91±3.32		
Overall survival event, n (%)						
Alive	8 (18.60)	8 (18.60)	0.043[b]	4.88±2.87	2.11	0.041
Dead	5 (11.63)	22 (51.16)		7.11±3.61		
Median age (interquartile range), years	48 (44-52)	51.5 (34.5-62.25)	0.339[c]			

[a]Pearson's χ^2 test; [b]Fisher's exact test; [c]Mann-Whitney U-test.

and conventional treatment, most patients have succumbed to this tumour within 2 years of diagnosis owing to recurrence and drug resistance (30). Furthermore, the presence of molecular heterogeneity and different tumour microenvironments (TMEs) within gliomas markedly affects patient prognosis and treatment response. Glioma cells actively interact with surrounding healthy cells and the immune milieu, thereby promoting tumour onset and progression (31). Innovative strategies to detect and treat gliomas can be derived by identifying critical molecules that communicate with the surrounding microenvironment or are implicated in TME formation.

The S100A6 protein belongs to group A of the calcium-binding S100 protein family. It is an intracellular protein and is associated with the modulation of several cellular activities, including proliferation, apoptosis, cytoskeleton dynamics and cellular responses to various stress factors (32). S100A6 and its ligands are widely expressed in neurons and astrocytes and may promote neuropathological progression when their expression is altered (32). Inhibition of its expression can be a new therapeutic approach for treating gliomas. Notably, S100A6 enhances the proliferation, migration, invasiveness and adhesion of malignant cells in breast, gastric, pancreatic and colon cancers (33,34) and is correlated with patient prognosis (35). In the present study, by analysing

TCGA data, the present authors noted that S100A6 expression was remarkably increased in glioma tissues compared with that in normal tissues. ROC diagnostic curves directly revealed that S100A6 can identify gliomas, thereby highlighting its diagnostic significance. As it is well known, IDH, as a recognized diagnostic marker for glioma, has excellent diagnostic efficacy (9). Meta-analysis showed that the AUC of IDH in the validation set can reach 0.89 (36). By contrast, as a new diagnostic marker, the diagnostic efficacy of s100A6 is still acceptable.

In addition, S100A6 expression exhibited a strong positive association with WHO grading, pathological stage and molecular markers such as IDH status and 1p/19q codeletion; this finding indicates that S100A6 is closely associated with tumorigenesis and progression, which was verified in clinical glioma samples. In gliomas, the presence of both 1p/19q codeletion and IDH mutations suggests a good prognosis and increased sensitivity to radiotherapy and chemotherapy (37,38). Based on these findings, we hypothesized that S100A6 can be used as an indicator for tumour staging in gliomas. Moreover, it was observed that patients with low S100A6 expression had a longer survival time than those with high expression. In addition, S100A6 independently functions as a risk predictor of OS in patients with glioma. Using a nomogram, the complex

Table II. Univariate analysis of OS.

Characteristic	Cases, n	Median survival (± standard deviation), months	95% CI, months	P-value
Age, years				
≤60	14	36.10±8.54	19.36-52.84	0.007
>60	6	13.17±4.51	4.32-22.02	
Sex				
Female	11	39.50±13.76	12.53-66.47	0.147
Male	9	29.73±11.52	7.15-52.32	
WHO grade				
G2	2	45.00		0.001
G3	7	48.00±1.31	45.43-50.57	
G4	11	22.00±4.70	12.80-31.20	
IDH status				
Wild type	9	22.00±12.37	0.00-46.25	0.003
Mutant	11	47.00±6.68	33.91-60.09	
1p/19q codeletion				
Codel	9	47.00±2.98	41.16-52.84	0.044
Non-codel	11	22.00±4.41	13.35-30.65	
S100A6 expression				
High	15	22.00±3.74	14.68-29.32	0.030
Low	5	47.00±2.19	42.71-51.29	

Cox regression model was transformed into a visual graph, increasing the readability of the results of the prediction model; it intuitively revealed the contribution of four factors, namely S100A6 expression, primary treatment outcomes, IDH status and WHO grade, in predicting patient prognosis and facilitated the clinical evaluation and prognosis management of patients with glioma. Therefore, taken together, the present findings suggest that S100A6 serves as a novel biomarker for the unfavourable prognosis of patients with glioma. Although nomograms can be used to assist decision-making, they also have certain limitations, such as being challenging in conveying relevant concepts to patients and the high theoretical nature of nomograms not fully representing good clinical effects. Therefore, it is necessary to have a comprehensive understanding of clinical issues and improve the performance of the nomogram to improve its application in the clinical decision-making process.

Analyses of the DEGs and expression-related gene enrichment of S100A6 in patients with glioma in the TCGA database revealed that S100A6 is primarily involved in immune responses, particularly in the activation of neutrophils and neutrophil-mediated immunity. Previous studies reported that the S100 family proteins can promote the migration and chemotaxis of immune cells and release several inflammatory cytokines and regulate inflammation and immune responses (11). In addition, S100A6 is generally detected at inflammatory sites (39). Tong *et al* (40) confirmed that S100A6 can induce *in vitro* inflammation by activating Kupffer cells, resulting in liver damage. Therefore, we hypothesize that the immune regulatory effect of S100A6 is an essential factor affecting glioma progression. Furthermore,

enrichment analysis revealed that S100A6 is related to chemical signal transmission and intercellular communication. In general, S100A6 plays an extracellular or intracellular role by interacting with binding or target proteins and activating downstream signalling pathways. Previous studies reported that S100A6 overexpression can increase β-catenin expression and nuclear translocation (13,15,31-41). β-Catenin is a key mediator involved in the canonical Wnt signalling pathway and transcriptional regulation of several genes (42). S100A6 can promote tumour cell growth and migration by activating extracellular regulated protein kinases 1/2 and p38/MAPKs in colorectal cancer. Another study suggested that S100A6 promotes nasopharyngeal carcinoma development by activating the p38/MAPK signalling pathway. Therefore, S100A6, a key mediator of signal transduction in tumours, may play a vital role in glioma occurrence and progression. In the future, the signalling pathways involved and specific mechanisms underlying S100A6 in glioma will be explored.

The tumour immune microenvironment is a critical factor associated with cancer onset and progression (43,44). Stromal cells in the TME and immune cells directly or indirectly affect the TME and regulate tumour cell behaviour. The TME has exerted a remarkable effect in clinical settings by facilitating the accurate anticipation of the prognosis and treatment response of patients with cancer (45,46). In the present study, increased S100A6 expression was significantly correlated with immune cell infiltration in the TME of patients with glioma. Compared with other tumour types, the TME of glioma is abundant in macrophages; these macrophages are generally polarized into tumour-supporting and immunosuppressive phenotypes (47); these macrophage phenotypes can

promote tumour cell bioactivity by releasing growth factors and cytokines (48,49) and correlate with the immunosuppressive phenotype of the TME (50). The present study found a positive association between S100A6 expression in glioma and macrophages, suggesting the role of S100A6 in the formation of a tumour-suppressive immune microenvironment in glioma. Chronic inflammation in the brain may induce mitochondrial dysfunction in gliomas and inhibit glioma cell apoptosis, thereby promoting tumour progression (27). Furthermore, tumour cells can evade the immune system by promoting ligand shedding of NK cell-activating receptors, upregulating the expression of inhibitory receptor ligands (51) and inhibiting the maturation of antigen-presenting cells (52). S100A6 expression in glioma was proven to be associated with the number of macrophages and other inflammatory cells in the tumour. S100A6 can significantly contribute to the modulation of tumour immunity and can be implicated in the formation of an immunosuppressive microenvironment in gliomas, which, in turn, promotes tumour growth.

Compared with the study of Zhang *et al* (20), both the present study and their study explored the expression, functional enrichment and relationship with immune cell infiltration of S100A6 in glioma. Nevertheless, the present study has a certain degree of innovation. Compared with others, the present study effectively verified the clinical significance of S100A6 in a small glioma cohort, explored the correlation between S100A6 protein levels and clinicopathological features and confirmed the clinical diagnostic value of S100A6 in distinguishing low- and high-grade gliomas. In addition, in the present study, the follow-up period was ~60 months. The present study obtained the complete survival data of patients and confirmed that S100A6 has a relatively stable prognostic significance in the clinical cohort. Therefore, the present study provides a good reference value and practical significance for promoting S100A6 as an effective molecular marker for glioma and the clinical management of patients with glioma in the future. However, the present study has some limitations. First, empirical data accessible in the public databases were lacking and contaminated tissues may have resulted in biased outcomes. Second, owing to the availability of a limited number of clinical samples, adequate clinical evidence could not be provided to fully confirm that S100A6 is an independent predictive factor for glioma; this should be validated in future clinical trials.

In summary, the present study found that enhanced expression of the S100A6 gene is linked to the unfavorable OS in glioma patients. We hypothesized that S100A6 would be useful as both a prognostic biological marker and as an indicator in the diagnosis of glioma. The present findings revealed novel perspectives that may improve the detection and treatment of glioma patients.

Acknowledgements

Not applicable.

Funding

Authors' contributions

BH drafted the manuscript and carried out the IHC staining experiments. HZ, YX, and LS analyzed and interpreted the data. YQ and BH designed the study. YQ and BH confirm the authenticity of all the raw data. All authors read and approved the final version of the manuscript.

Availability of data and materials

The datasets used and/or analyzed during the current study are available from the corresponding author on reasonable request.

Ethics approval and consent to participate

Ethical approval was received for the study by the Clinical Research Ethics Committee of The Second Affiliated Hospital, Zhejiang University School of Medicine (approval no. 2021-0641; Hangzhou, China). Informed consent was waived by the Clinical Research Ethics Committee of The Second Affiliated Hospital, Zhejiang University School of Medicine. All methods were carried out in accordance with relevant guidelines and regulations.

Patient consent for publication

Not applicable.

Competing interests

The authors declare that they have no competing interests.

References

1. Ostrom QT, Price M, Neff C, Cioffi G, Waite KA, Kruchko C and Barnholtz-Sloan JS: CBTRUS statistical report: Primary brain and other central nervous system tumors diagnosed in the United States in 2015-2019. Neuro Oncol 24 (Suppl 5): S1-S95, 2022.
2. Wesseling P and Capper D: WHO 2016 classification of gliomas. Neuropathol Appl Neurobiol 44: 139-150, 2018.
3. Xu S, Tang L, Li X, Fan F and Liu Z: Immunotherapy for glioma: Current management and future application. Cancer Letters 476: 1-12, 2020.
4. Wen J, Chen W, Zhu Y and Zhang P: Clinical features associated with the efficacy of chemotherapy in patients with glioblastoma (GBM): A surveillance, epidemiology, and end results (SEER) analysis. BMC Cancer 21: 81, 2021.
5. Tan AC, Ashley DM, López GY, Malinzak M, Friedman HS and Khasraw M: Management of glioblastoma: State of the art and future directions. CA Cancer J Clin 70: 299-312, 2020.
6. Ramón Y Cajal S, Sesé M, Capdevila C, Aasen T, De Mattos-Arruda L, Diaz-Cano SJ, Hernández-Losa J and Castellví J: Clinical implications of intratumor heterogeneity: Challenges and opportunities. J Mol Med (Berl) 98: 161-177, 2020.
7. Binder DC, Ladomersky E, Lenzen A, Zhai L, Lauing KL, Otto-Meyer SD, Lukas RV and Wainwright DA: Lessons learned from rindopepimut treatment in patients with EGFRvIII-expressing glioblastoma. Transl Cancer Res 7 (Suppl 4): S510-S513, 2018.
8. Wick W, Gorlia T, Bendszus M, Taphoorn M, Sahm F, Harting I, Brandes AA, Taal W, Domont J, Idbaih A, *et al*: Lomustine and bevacizumab in progressive glioblastoma. N Engl J Med 377: 1954-1963, 2017.
9. de la Fuente MI, Colman H, Rosenthal M, Van Tine BA, Levacic D, Walbert T, Gan HK, Vieito M, Milhem MM, Lipford K, *et al*: Olutasidenib (FT-2102) in patients with relapsed or refractory IDH1-mutant glioma: A multicenter, open-label, phase Ib/II trial. Neuro Oncol 25: 146-156, 2023.

10. Bale TA and Rosenblum MK: The 2021 WHO classification of tumors of the central nervous system: An update on pediatric low-grade gliomas and glioneuronal tumors. Brain Pathol 32: e13060, 2022.
11. Gonzalez LL, Garrie K and Turner MD: Role of S100 proteins in health and disease. Biochim Biophys Acta Mol Cell Res 1867: 118677, 2020.
12. Li Z, Tang M, Ling B, Liu S, Zheng Y, Nie C, Yuan Z, Zhou L, Guo G, Tong A and Wei Y: Increased expression of S100A6 promotes cell proliferation and migration in human hepatocellular carcinoma. J Mol Med (Berl) 92: 291-303, 2014.
13. Li Y, Wagner ER, Yan Z, Wang Z, Luther G, Jiang W, Ye J, Wei Q, Wang J, Zhao L, *et al*: The calcium-binding protein S100A6 accelerates human osteosarcoma growth by promoting cell proliferation and inhibiting osteogenic differentiation. Cell Physiol Biochem 37: 2375-2392, 2015.
14. Chen X, Liu X, Lang H, Zhang S, Luo Y and Zhang J: S100 calcium-binding protein A6 promotes epithelial-mesenchymal transition through β-catenin in pancreatic cancer cell line. PLoS One 10: e0121319, 2015.
15. Wang XH, Zhang LH, Zhong XY, Xing XF, Liu YQ, Niu ZJ, Peng Y, Du H, Zhang GG, Hu Y, *et al*: S100A6 overexpression is associated with poor prognosis and is epigenetically up-regulated in gastric cancer. Am J Pathol 177: 586-597, 2010.
16. Li L, Pan Y, Mo X, Wei T, Song J, Luo M, Huang G, Teng C, Liang K, Mao N and Yang J: A novel metastatic promoter CEMIP and its downstream molecular targets and signaling pathway of cellular migration and invasion in SCLC cells based on proteome analysis. J Cancer Res Clin Oncol 146: 2519-2534, 2020.
17. Camby I, Nagy N, Lopes MB, Schäfer BW, Maurage CA, Ruchoux MM, Murmann P, Pochet R, Heizmann CW, Brotchi J, *et al*: Supratentorial pilocytic astrocytomas, astrocytomas, anaplastic astrocytomas and glioblastomas are characterized by a differential expression of S100 proteins. Brain Pathol 9: 1-19, 1999.
18. Camby I, Lefranc F, Titeca G, Neuci S, Fastrez M, Dedecken L, Schäfer BW, Brotchi J, Heizmann CW, Pochet R, *et al*: Differential expression of S100 calcium-binding proteins characterizes distinct clinical entities in both WHO grade II and III astrocytic tumours. Neuropathol Appl Neurobiol 26: 76-90, 2000.
19. Kucharczak J, Pannequin J, Camby I, Decaestecker C, Kiss R and Martinez J: Gastrin induces over-expression of genes involved in human U373 glioblastoma cell migration. Oncogene 20: 7021-7028, 2001.
20. Zhang Y, Yang X, Zhu XL, Bai H, Wang ZZ, Zhang JJ, Hao CY and Duan HB: S100A gene family: Immune-related prognostic biomarkers and therapeutic targets for low-grade glioma. Aging (Albany NY) 13: 15459-15478, 2021.
21. Blum A, Wang P and Zenklusen JC: SnapShot: TCGA-analyzed tumors. Cell 173: 530, 2018.
22. Chin L, Hahn WC, Getz G and Meyerson M: Making sense of cancer genomic data. Genes Dev 25: 534-555, 2011.
23. Grossman RL, Heath AP, Ferretti V, Varmus HE, Lowy DR, Kibbe WA and Staudt LM: Toward a shared vision for cancer genomic data. N Engl J Med 75: 1109-1112, 2016.
24. Ceccarelli M, Barthel FP, Malta TM, Sabedot TS, Salama SR, Murray BA, Morozova O, Newton Y, Radenbaugh A, Pagnotta SM, *et al*: Molecular profiling reveals biologically discrete subsets and pathways of progression in diffuse glioma. Cell 164: 550-663, 2016.
25. Love MI, Huber W and Anders S: Moderated estimation of fold change and dispersion for RNA-seq data with DESeq2. Genome Biol 15: 550, 2014.
26. Yan X, Hong B, Feng J, Jin Y, Chen M, Li F and Qian Y: B7-H4 is a potential diagnostic and prognostic biomarker in colorectal cancer and correlates with the epithelial-mesenchymal transition. BMC Cancer 22: 1053, 2022.
27. Fan W, Song Y, Ren Z, Cheng X, Li P, Song H and Jia L: Glioma cells are resistant to inflammation-induced alterations of mitochondrial dynamics. Int J Oncol 57: 1293-1306, 2020.
28. Liu J, Lichtenberg T, Hoadley KA, Poisson LM, Lazar AJ, Cherniack AD, Kovatich AJ, Benz CC, Levine DA, Lee AV, *et al*: An integrated TCGA pan-cancer clinical data resource to drive high-quality survival outcome analytics. Cell 173: 400-416.e411, 2018.
29. Yu CH: Evaluation of diagnostic test. Medical statistics. Beijing: People's Medical Publishing House 164-178, 2002. (In Chinese).
30. Radin DP, Tsirka SE: Interactions between tumor cells, neurons, and microglia in the glioma microenvironment. Int J Mol Sci 21: 8476, 2020.
31. Barthel L, Hadamitzky M, Dammann P, Schedlowski M, Sure U, Thakur BK and Hetze S: Glioma: molecular signature and crossroads with tumor microenvironment. Cancer Metastasis Rev 41: 53-75, 2022.
32. Filipek A and Leśniak W: S100A6 and its brain ligands in neurodegenerative disorders. Int J Mol Sci 21: 3979, 2020.
33. Donato R, Sorci G and Giambanco I: S100a6 protein: functional roles. Cell Mol Life Sci 74: 2749-2760, 2017.
34. Hua X, Zhang H, Jia J, Chen S, Sun Y and Zhu X: Roles of S100 family members in drug resistance in tumors: Status and prospects. BioMed Pharmacother 127: 110156, 2020.
35. Hu Y, Zeng N, Ge Y, Wang D, Qin X, Zhang W, Jiang F and Liu Y: Identification of the shared gene signatures and biological mechanism in type 2 diabetes and pancreatic cancer. Front Endocrinol (Lausanne) 13: 847760, 2022.
36. Zhao J, Huang Y, Song Y, Xie D, Hu M, Qiu H and Chu J: Diagnostic accuracy and potential covariates for machine learning to identify IDH mutations in glioma patients: Evidence from a meta-analysis. Eur Radiol 30: 4664-4674, 2020.
37. Ghouzlani A, Kandoussi S, Tall M, Reddy KP, Rafii S and Badou A: Immune checkpoint inhibitors in human glioma microenvironment. Front Immunol 12: 679425, 2021.
38. Lapointe S, Perry A and Butowski NA: Primary brain tumours in adults. Lancet 392: 432-446, 2018.
39. Wirths O, Breyhan H, Marcello A, Cotel MC, Bruck W and Bayer TA: Inflammatory changes are tightly associated with neurodegeneration in the brain and spinal cord of the APP/PS1KI mouse model of Alzheimer's disease. Neurobiol Aging 31: 747-757, 2010.
40. Tong H, Wang L, Zhang K, Shi J, Wu Y, Bao Y and Wang C: Correction to: S100A6 activates kupffer cells via the p-P38 and p-JNK pathways to induce inflammation, mononuclear/macrophage infiltration sterile liver injury in mice. Inflammation 46: 555, 2023.
41. Liu Z, Zhang X, Chen M, Cao Q and Huang D: Effect of S100A6 over-expression on beta-catenin in endometriosis. J Obstet Gynaecol Res 41: 1457-1462, 2015.
42. Rijsewijk F, van Deemter L, Wagenaar E, Sonnenberg A and Nusse R: Transfection of the int-1 mammary oncogene in cuboidal RAC mammary cell line results in morphological transformation and tumorigenicity. EMBO J 6: 127-131, 1987.
43. Deberardinis RJ: Tumor microenvironment, metabolism, and immunotherapy. N Engl J Med 382: 869-871, 2020.
44. Chen F, Song J, Ye Z, Xu B, Cheng H, Zhang S and Sun X: Integrated analysis of cell cycle-related and immunity-related biomarker signatures to improve the prognosis prediction of lung adenocarcinoma. Front Oncol 11: 666826, 2021.
45. Li C, Jiang P, Wei S, Xu X and Wang J: Regulatory T cells in tumor microenvironment: New mechanisms, potential therapeutic strategies and future prospects. Mol Cancer 19: 116, 2020.
46. Erin N, Grahovac J, Brozovic A and Efferth T: Tumor microenvironment and epithelial mesenchymal transition as targets to overcome tumor multidrug resistance. Drug Resist Update 53: 100715, 2020.
47. Wei J, Chen P, Gupta P, Ott M, Zamler D, Kassab C, Bhat KP, Curran MA, de Groot JF and Heimberger AB: Immune biology of glioma-associated macrophages and microglia: Functional and therapeutic implications. Neuro Oncol 22: 180-194, 2020.
48. Xia Y, Rao L, Yao H, Wang Z, Ning P and Chen X: Engineering macrophages for cancer immunotherapy and drug delivery. Adv Mater 32: e2002054, 2020.
49. Hambardzumyan D, Gutmann DH and Kettenmann H: The role of microglia and macrophages in glioma maintenance and progression. Nat Neurosci 19: 20-27, 2016.
50. Domingues P, González-Tablas M, Otero Á, Pascual D, Miranda D, Ruiz L, Sousa P, Ciudad J, Gonçalves JM, Lopes MC, *et al*: Tumor infiltrating immune cells in gliomas and meningiomas. Brain Behav Immun 53: 1-15, 2016.
51. Di W, Fan W, Wu F, Shi Z, Wang Z, Yu M, Zhai Y, Chang Y, Pan C, Li G, *et al*: Clinical characterization and immunosuppressive regulation of CD161 (KLRB1) in glioma through 916 samples. Cancer Sci 113: 756-769, 2022.
52. Cho A, McKelvey KJ, Lee A and Hudson AL: The intertwined fates of inflammation and coagulation in glioma. Mamm Genome 29: 806-816, 2018.